

HFIP-assisted Brønsted acid-catalyzed ring opening of 1-azabicyclo[1.1.0]butane to access diverse C3-quaternary aza-azetidines and indole-azetidines

Received: 26 February 2025

Accepted: 26 August 2025

Published online: 30 September 2025

Subrata Hazra¹, Arushi Tyagi², Tuhin Dutta³, Rupam Sahoo¹,
Boudhayan Bandyopadhyay³, Garima Jindal² & Santanu Panda¹✉

Nitrogen-based heterocycles represent 60% of small-molecule-approved drugs. Increasing demand for sp^3 -rich *N*-heterocyclic scaffolds as a bioisosteric replacement in drug discovery platforms has continued to drive the development of elegant methods for the synthesis of these important molecules. Among various *N*-heterocycles, azetidine has emerged as a valuable scaffold. Aza-azetidines, indole-azetidines, and spirocyclic azetidines with tertiary or quaternary C3-carbon make structural and/or functional parts of various important drug molecules. However, an efficient and catalytic synthetic strategy to access those important scaffolds is still missing in the literature. Herein, we report HFIP-assisted Brønsted acid-catalyzed strain-release driven ring opening of 1-azabicyclo[1.1.0]butane (ABB) to access aza-azetidines, indole-azetidines, and spirocyclic azetidines with quaternary C3-carbon in good yield. Detailed experimental and theoretical studies using DFT shed light on the reaction mechanism. We also find promising antibacterial activity in one of these indole-azetidine compounds against *Staphylococcus aureus* MTCC 1430.

Scaffold hopping refers to the swapping of isofunctional molecular structures with completely different core structures to improve potency and mitigate the problems related to toxicity, stability, and other physicochemical properties^{1–3}. Scaffold hopping by bioisosteric replacement has proven to be a very successful strategy for lead generation^{4,5}. Recently, there has been a lot of interest in bioisosteric replacement of small, strained sp^3 -rich *N*-heterocycles into various molecular frameworks, as these fragments have the potential to provide favorable pharmacological properties without substantially increasing the overall molecular weight^{6,7}. Azetidines have emerged as privileged structural motifs in pharmaceutical and agrochemical drug discovery campaigns; they can resemble pyridine, piperidine, and

pyrrolidine for bioisosteric replacement^{8,9}. Among the functionalized azetidine frameworks, the aza-azetidine, indole-azetidine, and azetidine with spirocyclic rings have huge importance in medicinal chemistry^{8,10–12}. Aza-azetidine is known as a bioisostere of piperazine (Fig. 1a)^{13,14}, which is an important *N*-heterocycle found in hundreds of marketed drugs¹⁵. Most importantly, the bioisosteric replacement of piperazine by aza-azetidine has shown a huge improvement in biological activity¹⁶. In this respect, it has become very important to develop a better strategy for the construction of aza-azetidine in an efficient manner. Because of the similarity in their physical and chemical properties, we hypothesized that indole-azetidine could be a bioisostere of tryptamine (Fig. 1b), an indolamine metabolite present in a large

¹Department of Chemistry, Indian Institute of Technology Kharagpur, Kharagpur, India. ²Department of Organic Chemistry, Chemical Science Division, Indian Institute of Science, Bangalore, India. ³Department of Biotechnology, School of Life Science and Biotechnology, Adamas University, Kolkata, India.

✉ e-mail: panda.santanu@gmail.com

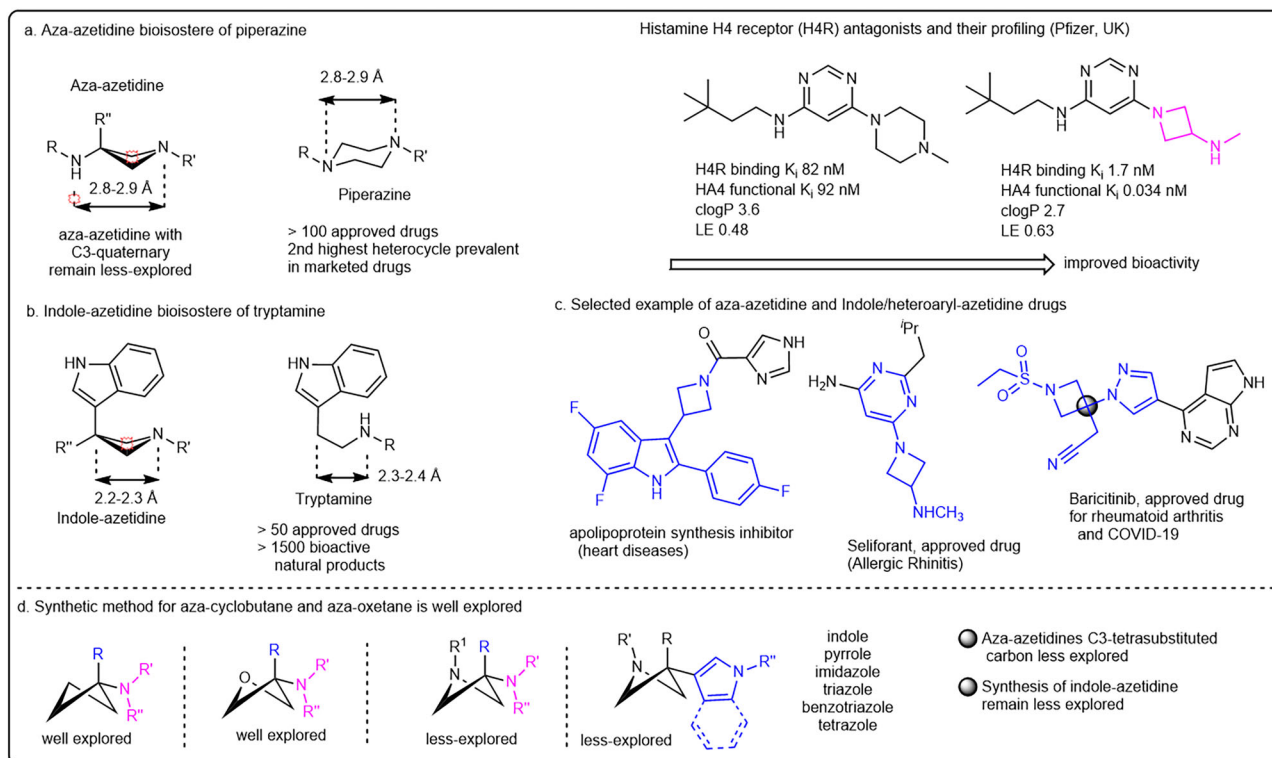


Fig. 1 | Background and conceptual design. a Aza-azetidine bioisostere of piperazine. **b** Indole-azetidine bioisostere of tryptamine. **c** Selected examples of aza-azetidine and indole/heteroaryl-azetidine drugs. **d** Synthetic method for aza-cyclobutane and aza-oxetane is well explored.

number of lifesaving drugs and natural products¹⁷. Aza-azetidine and indole-azetidines are present in many marketed drugs and bioactive compounds (Fig. 1c). Recently, several strategies for the synthesis of aza-cyclobutane and aza-oxetane have been documented^{18–20}. However, a general approach to access diverse aza-azetidine, indole- and other *N*-heterocyclic azetidine with a C3 quaternary center is still remains unexplored (Fig. 1d). Despite their importance, the synthesis process is often encumbered by the limited number of efficient, robust methods to access these drug-like molecules^{10,21–28}.

The 1-azabicyclo[1.1.0]butane (ABB), a strained bicyclic structure consisting of two carbon atoms forming a bridge and another carbon atom forming a bond with a nitrogen atom, has been known for synthesizing diverse azetidines^{29–31}. Strong nucleophiles are known to cleave the internal C–N bond by directly attacking the bridgehead carbon to form C3-substituted azetidines³¹. Strong acids are also known to open up the ABB ring in the presence of nucleophilic counter anions³². Other strategies like sequential ring-opening and C-functionalization³³ or *N*-functionalization³⁴, [2 + 2] cycloaddition³⁵, Buchwald–Hartwig coupling after carbonyl functionalization using strong nucleophiles³⁶, or acylation/sulfonylation, were also reported for the synthesis of azetidines. The Aggarwal and the Saha group explored 3-lithiated ABBs as nucleophiles in the modular synthesis of azabicyclo[1.1.0]butyl carbinols and activation of the nitrogen-atom using trifluoroacetic anhydride or aza-oxyallyl cations, respectively, to access C3 and *N*-substituted azetidines^{21,22,37,38}. Recently, the radical-induced ring opening of ABBs was explored using sulfonyl imine in the presence of an organic photosensitizer³⁹.

In terms of aza-azetidine synthesis, the pioneering work was reported from the Młostoń group, which goes via ring opening of ABB using hydrazoic acid, followed by Raney nickel-catalyzed reduction of azide to amine⁴⁰. Later, the Baran group introduced the strain-released driven ring opening of ABBs using turbo amide (Fig. 2a)^{23,24}. Recently, the Rousseaux group reported nickel-catalyzed cross-coupling of Boc-

protected azetidine-3-amino-*N*-hydroxyphthalimide with aryl halide for the synthesis of aza-azetidine²⁵, where the synthesis of azetidine-*N*-hydroxyphthalimide was achieved in seven linear steps starting from commercially available compounds (Fig. 2a)²⁶. Only very recently, Dell’Amico group reported the strain-driven photocatalyzed sulfoimination of ABBs using sulfonyl imine as the reaction partner, which was later hydrolyzed to aza-azetidines (Fig. 2a)³⁹. The Bull group developed a unique defluorosulfonylation reaction pathway (deFS) to access azetidine sulfonyl fluorides in five steps starting from the 3-keto azetidine, which can be further converted to aza-azetidine by reacting with a neutral amine under thermal conditions (Fig. 2a)²⁷. While these approaches work well for several amines, the reactivity with anilines remains unexplored.

Similarly, we can find a five-step strategy to access indole-azetidine starting from indole and 3-keto azetidine, which goes via protection of indole, C3-lithiation, addition to *N*-Boc-3-keto azetidine, removal of the hydroxyl group with Boc-deprotection, and finally reductive amination (Fig. 2b)¹⁰. We also find a single example in the recently published work from the Aggarwal²¹ and Saha group^{22,28}, where the indole-azetidine was synthesized from indole-ABB-carbinol after electrophile-activated semipinacol rearrangement. Despite a few reports, a general synthetic strategy to access C3-quaternary indole-azetidines using indole as a nucleophilic precursor is still in its infancy and requires further development and validation.

The use of Brønsted acid catalysis in HFIP gained a lot of interest due to its unique activation profile, and less is known about its activation profile, which mostly depends on the particular reaction^{41–47}. We hypothesized that the catalytic amount of Brønsted acid in the HFIP solvent might activate both the nitrogen atom of the azetidine ring and the benzoyl oxygen atom at the C3 position. A double activation strategy will create a delta positive charge on the C3-carbon for successful ring opening in the presence of indoles, anilines, and other *N*-heteroaryl compounds.

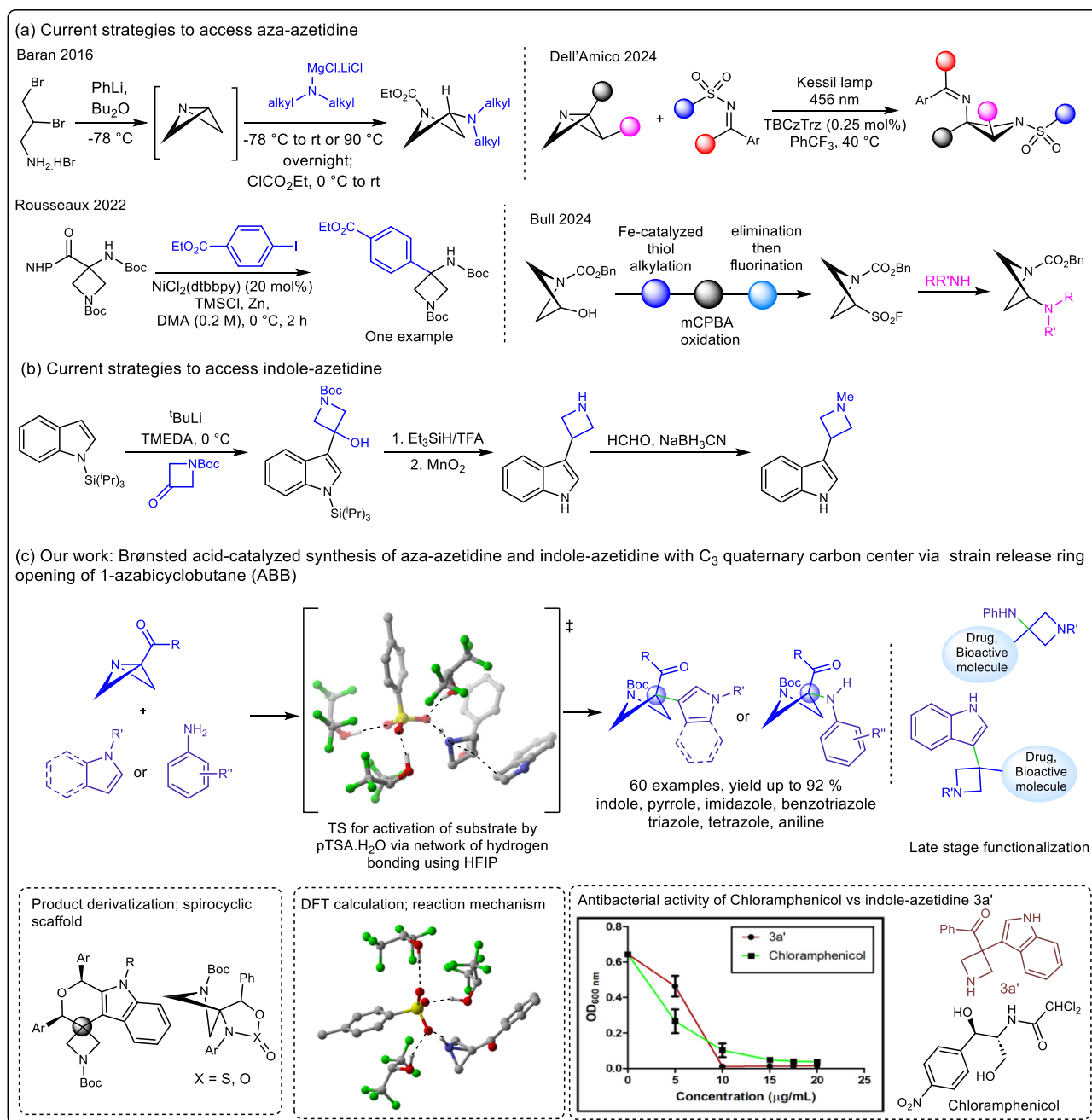


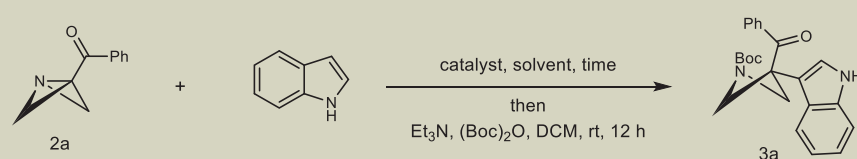
Fig. 2 | Literature vs our work. a Current strategies to access aza-azetidine. **b** Current strategies to access indole-azetidine. **c** Brønsted acid-catalyzed synthesis of aza-azetidine and indole-azetidine with C₃ quaternary carbon center via strain release ring opening of ABB.

Herein, we report a hydrogen bonding-assisted Brønsted acid-catalyzed strain release-driven ring opening of benzoylated ABB ring using anilines, indoles, and other *N*-heteroaryl to access a large number of C₃-quaternary aza-azetidine, indole-azetidine in excellent yield (Fig. 2c). Further, the aza-azetidine or indole-azetidine can be converted to an important class of azetidine-based spirocyclic compounds. The aza-azetidine or indole-azetidine core was introduced to various marketed drugs and bioactive molecules, which can expedite the future fragment-based drug discovery approach. The reaction mechanism was supported by detailed DFT calculations, as well as in situ NMR studies. Finally, in collaboration with the Bandyopadhyay group, we tested the antibacterial activity of these compounds, and we are excited to find a potential antibacterial agent against the tested gram-positive bacteria, i.e., *Staphylococcus aureus* MTCC 1430, which is discussed in detail in the later section.

Results and discussion

Reaction optimization

We initiated our studies with the synthesis of benzoylated ABB substrate starting from 2,3-dibromopropan-1-amine hydrobromide, following a literature-reported procedure²². First, it goes via lithiation of 2,3-dibromopropan-1-amine using *sec*-BuLi at -78°C , followed by the addition of Weinreb amide. Several benzoylated ABB have been synthesized by following this strategy. Also, we have introduced the ABB ring in various bioactive molecules, marketed drugs, fatty acids, and bile acids (see the Supplementary Information, Section 3 for more details). Next, we initiated our optimization study with benzoylated ABB (**2a**) and indole in the presence of various Brønsted acids and Lewis acids to open the ABB ring and further in situ Boc-protection of the nitrogen atom. Initially, we screened various

Table 1 | Optimization study


Entry	Solvent	Catalyst	Time	Temperature	Yield of 3a (%)
1	DCM	HCl	24 h	rt	0
2	DCM	H ₃ PO ₄	24 h	rt	0
3	DCM	PhCO ₂ H	24 h	rt	0
4	DCM	TFA	24 h	rt	0
5	DCM	pTSA.H ₂ O	24 h	rt	0
6	DCM	ZnBr ₂	24 h	rt	0
7	DCM	Cu(OTf) ₂	24 h	rt	0
8	DCM	Zn(OTf) ₂	24 h	rt	0
9	DCM	Sc(OTf) ₃	24 h	rt	Trace
10	MeCN	pTSA.H ₂ O	24 h	rt	0
11	DMF	pTSA.H ₂ O	24 h	rt	Trace
12	DMSO	pTSA.H ₂ O	24 h	rt	trace
13	EtOH	pTSA.H ₂ O	24 h	rt	0
14	^t PrOH	pTSA.H ₂ O	24 h	rt	0
15	TFE	pTSA.H ₂ O	24 h	rt	15
16	HFIP	pTSA.H ₂ O	24 h	rt	85
17 ^b	HFIP	pTSA.H ₂ O	24 h	rt	78
18 ^c	HFIP	pTSA.H ₂ O	24 h	rt	75
19	HFIP	-	24 h	rt	20

^aReaction condition: 2a (0.2 mmol), indole (0.4 mmol), catalyst (10 mol%), HFIP (0.2 mL); after removal of HFIP add Et₃N (0.8 mmol), Boc₂O (0.4 mmol), DCM (5 mL).

^bpTSA.H₂O (5 mol%).

^cpTSA.H₂O (20 mol%).

^dAll yields are isolated yields after Boc-protection. For more optimization studies, see Supplementary Information, Table S1.

Brønsted acids and Lewis acids, keeping DCM as solvent (Table 1, entries 1–9). But we did not find any success under those conditions. Then we thought to introduce Brønsted acids to activate ABB via protonation. From the literature, pTSA.H₂O is known as a very good Brønsted acid with a non-nucleophilic counter anion. So, we decided to screen 10 mol% pTSA.H₂O as a catalyst in the presence of various polar-aprotic and polar-protic solvents. Such solvent screening leads to either trace or no yield of the desired product under both ambient temperature and reflux conditions (Supplementary Information, Table S1, entries 14–23). Finally, in trifluoroethanol (TFE), we got the desired product in 15% isolated yield after 24 h of reaction (Table 1, entry 15). This data indicates that the hydrogen bonding ability of the reaction solvent plays an important role. By introducing HFIP as a solvent, we observed full conversion of the starting material after 24 h, and the desired product was isolated with 85% yield (Table 1, entry 16). Decreasing or increasing the catalyst loading had a detrimental effect on the isolated yield (Table 1, entries 17 and 18). Lowering the reaction time or equivalent of indole leads to a further decrease in yield (Supplementary Information, Table S1, entries 28–31). In the absence of any Brønsted acid, only 20% yield of the desired product was observed (Table 1, entry 19). This is due to the acidity of the solvent itself. HFIP can form a strong hydrogen bond with the ABB nitrogen atom and can activate the substrate to some extent. Although this barrier was found to be high (30.6 kcal/mol) (see Supplementary Information, Section 20). Further screening of other Brønsted acids did not improve the yield (Supplementary Information, Table S1, entries 33–38). We observed the decomposition of the starting material in many cases with messy reactions. Also, the benzoyl group at the C3 position is found to be critical to achieve a good yield of the desired product.

Synthesis of C3-quaternary indole-azetidine

Having the optimized condition in hand, we started exploring the generality of our method (Fig. 3). First, we screened differently substituted indoles along with benzoylated ABB (2a) as an electrophilic coupling partner. Indoles with substitution at different positions (3a–3f, 3x, 3y) are well tolerated, and all the indole-azetidines were isolated in good to excellent yield. The structure of the indole-azetidines was confirmed by the X-ray crystal structure of 3a. Also, the C2-substituted indole is compatible with this reaction, and the corresponding product was isolated in 71% yield after Boc-protection (3g). Not only free indole, *N*-protected indoles such as *N*-methyl and *N*-benzyl indole also react with 2a to form the desired product (3h and 3i) in 78% and 72% yield, respectively. After a successful exploration of the indole scope, we also explored the generality of benzoylated ABB. Various benzoylated ABB-bearing electron-donating and electron-withdrawing substituents react with indole to form the corresponding indole-azetidines in good yield (3j–3m, 3z). Benzoylated ABB with electron-donating substituents leads to comparatively lower yields than with electron-withdrawing substituents, which explains the adverse effect of the electron-donating group on the phenyl ring. Also, α -naphthoylated and α -thenoylated ABB undergo nucleophilic ring opening to form the corresponding products (3n and 3o) in good yields. However, pivaloylated ABB leads to a moderate yield of 42% (3p) could be due to steric reasons. After successfully exploring the indole-azetidine scopes, we shift our attention towards other nitrogen-based heterocycles. Under the standard pTSA.H₂O condition, the reaction of benzoylated ABB (2a) with pyrrole, *N*-methyl pyrrole, and imidazole is very slow and only leads to trace amounts of desired products even after 24 h. But, in the presence of 10 mol% TFA, they do

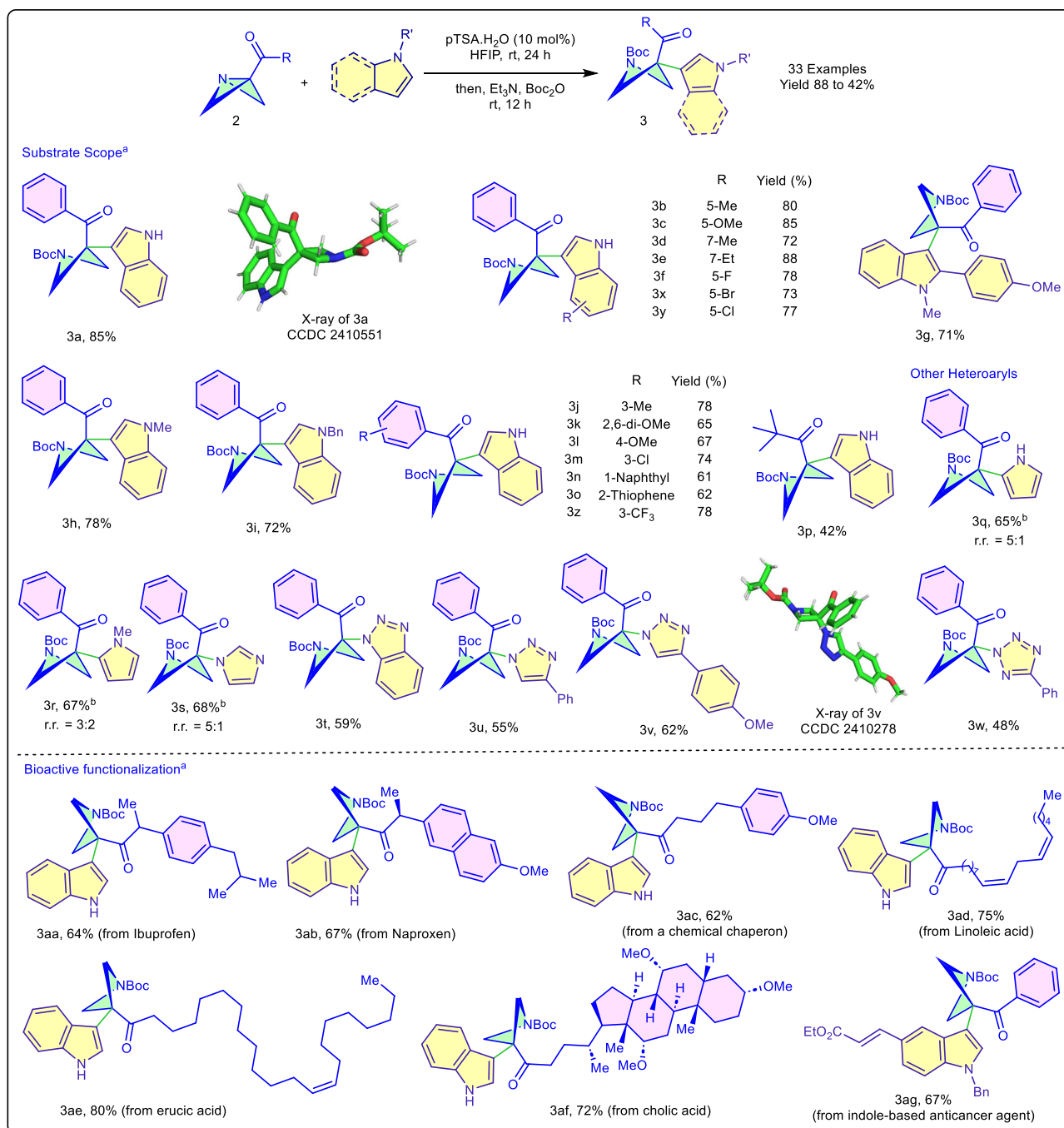


Fig. 3 | Substrate scope for nucleophilic ring opening of ABB using indole and other *N*-heterocycles; installation of indole-azetidine in bioactive molecules, marketed drugs, and fatty acids. [a] Reaction condition: **2 (0.2 mmol), nucleophile (0.4 mmol), pTSA.H₂O (10 mol%), HFIP (0.2 mL), after removal of HFIP add**

Et₃N (0.8 mmol), Boc₂O (0.4 mmol), DCM (5 mL). [b] TFA (10 mol%) instead of pTSA.H₂O. The regioisomeric ratio (*r.r.*) was determined from the ¹H NMR integration values.

react with **2a** to form the desired product in good yield. Pyrrole can undergo electrophilic substitution both at C2 and C4 (C3'), although C2 is a more reactive position. This is also reflected in our results; in the case of pyrrole, we also observed a mixture of regioisomeric products with *r.r.* 5:1 (**3q**). In the case of *N*-methyl pyrrole, the *r.r.* is 3:2 (**3r**); although the regioisomers are separable, we have isolated both regioisomers and characterized them. In the case of imidazole, we observed a mixture of *N*-substituted and *C*-substituted products with *r.r.* 5:1. However, benzotriazole and triazole react with **2a** under standard pTSA.H₂O conditions to form the corresponding aza-azetidines with good yield (**3t–3v**). In the case of benzotriazole, along with the

desired product, two sequential ring openings take place and form the byproduct **3t'** (Supplementary Information, Page S32). The structure of **3v** was confirmed by the X-ray crystal structure. Tetrazole also reacts under the optimal conditions to form the corresponding product in moderate yield (**3w**). We have also checked the reactivity of other heterocycles, such as furan, benzofuran, thiophene, benzothiofene, pyridine, etc., but they are found to be inert towards the nucleophilic ring opening of benzoylated ABB under both pTSA.H₂O and TFA conditions.

Inspired by the large substrate scope and functional group tolerance, we investigated the utility of our protocol towards the modular

installation of indole-azetidines in bioactive molecules, marketed drugs, fatty acids, etc. (Fig. 3). The nonsteroidal anti-inflammatory drugs (NSAID) ibuprofen and naproxen-based ABBs (**2i** and **2j**) react with indole to form the desired products (**3aa**, **3ab**) in 64% and 67% yield, respectively. Chemical chaperone-based ABB (**2k**) was also derivatized with a satisfactory yield of 62% (**3ac**). Interestingly, fatty acid-based ABBs such as linoleic acid-derived ABB (**2l**) and erucic acid-derived ABB (**2m**) are also found to be compatible with our reported protocol. Both products were isolated in very good yields of 75% and 80%, respectively (**3ad**, **3ae**). Finally, cholic acid (bile acid) based ABB (**2n**) was also found to react with indole to form the desired product in 72% yield (**3af**). Indole-based anticancer compound (**5S**)⁴⁸ can take part in the reaction with **2a** to form the desired **3ag** in 67% yield. Apart from the synthesis of these drug-like molecules, we have conducted a preliminary bioactivity study to showcase their potential as a future drug candidate, which will be discussed in the latter part of this manuscript.

Synthesis of C3-quaternary aza-azetidines

Aniline is the simplest aromatic amine and is used in the production of pharmaceuticals, dyes, and various other products. Considering that, we tried the strain-release-driven ring opening of benzoylated ABB (**2a**) with anilines, which remained unexplored (Fig. 4). Unfortunately, no desired product was formed when aniline was reacted with **2a** using our previously optimized conditions (pTSA.H₂O/HFIP). Again, we optimized the reaction conditions for aniline by screening various solvents and catalysts (see Supplementary Information, Table S2, page S17), and we found out that using 10 mol% TFA in HFIP solvent, the reaction occurs with full conversion within 2 h only. The nitrogen lone pair of aniline acts as a nucleophile to attack the C3-position of benzoylated ABB, followed by proton transfer, leading to the corresponding C3-quaternary aza-azetidines. Motivated by this result, we then started exploring the scope of the aniline (Fig. 4). Anilines with electron-donating and electron-withdrawing substituents at *ortho*-, *meta*-, and *para*-positions are well tolerated, and all the aza-azetidines obtained in good to excellent yield (**4a–4k**). 3-Ethynylaniline also undergoes the reaction to form the desired product with 83% yield, where the terminal alkyne moiety survives during the reaction (**4l**). Not only monosubstituted anilines, but disubstituted anilines were also found to be compatible during the reaction, and the corresponding C3-quaternary aza-azetidines were isolated in good to excellent yield (**4m–4o**). After the successful incorporation of different anilines, we investigated the benzoylated ABB scope for this reaction. Benzoylated ABB with electron-donating and electron-withdrawing substituents on the phenyl ring are also well executed (**4p–4s**, **4w**). Also, α -naphthoylated, α -thenoylated, and pivaloylated ABBs react with aniline to give the corresponding aza-azetidines with good to moderate yield (**4t–4v**). After the successful installation of indole-azetidines, we incorporated the aza-azetidines into biorelevant molecules such as marketed drugs, bioactive molecules, fatty acids, etc. (**4aa–4ah**) and isolated the desired products in good yield (Fig. 4). These results indicate the practicality of this methodology and its potential benefits for the drug design campaign.

Mechanistic investigations

To check the validity of the hydrogen bonding network between pTSA.H₂O and HFIP, we have performed a ¹H NMR perturbation study using HFIP and pTSA.H₂O (Fig. 5a). A fast proton exchange between pTSA and the hydroxyl proton of HFIP was observed. Similar to previous reports^{43,49}, we also observed a downfield shift of the combined acidic proton of pTSA and HFIP with the increasing amount of pTSA. Also, the ¹H and ¹³C NMR perturbation study of a 1:1 mixture of benzoylated ABB (**2a**) and HFIP supported the hydrogen bonding between the substrate and HFIP (Fig. 5b and Supplementary information, Section 12 for more details).

To have a better understanding of the strain release ring opening of benzoylated ABB, we have performed a series of control experiments. First, we have performed an indole-based nucleophilic ring opening of ABB (**2o** and **2p**) where the carbonyl group is absent (Fig. 5c). In that case, we got the desired products (**3ai** and **3aj**) only with 28% and 24% of isolated yield, respectively. This result signifies the importance of the carbonyl group, which acts as an electron-withdrawing group to facilitate the nucleophilic attack at the C3-position. 3-Methyl indole didn't give the desired product because of steric factors, and the aromatization step is not feasible in that case. Also, *N,N*-dimethyl aniline, and aliphatic primary amine didn't react with benzoylated ABB (**2a**) under the optimized conditions.

To elucidate the mechanism of the reaction, detailed DFT calculations were performed using benzoylated ABB (**2a**) and indole as model substrates using the SMD(HFIP)/M06-2X-D3/6-311+G**/M06-2X-D3/6-31G** level of theory (Fig. 5d). Based on the literature precedent, pTSA can bind with three molecules of HFIP to generate a catalytic triad⁴³, resulting in lowering the pK_a of pTSA compared to other solvents. We also considered that this catalytic triad is responsible for the protonation of the nitrogen atom of the benzoylated ABB ring, which we observed in our calculations done in an explicit solvent model. Protonation of the ABB ring generates **A_{pTSA-3HFIP}**, showing the free energy of protonation to be −2.0 kcal/mol (w.r.t. **A_{pTSA}**) (Fig. 5d). As it is evident from the bond distances between O1 and H1 in **A_{pTSA}** and **A_{pTSA-3HFIP}**, viz. 1.02 and 1.40 Å, respectively (Fig. 5e), the proton is closer to the nitrogen of ABB in **A_{pTSA-3HFIP}** than in **A_{pTSA}**, therefore activating the C3 position of ABB towards nucleophilic attack (Fig. 5e). The C3 position of indole is the most nucleophilic and thus attacks the C3 position of ABB, via **TS(A-B)_{pTSA}** (in the implicit solvent model) and **TS(A-B)_{pTSA-3HFIP}** (in the explicit solvent model) bearing activation free energies equal to 26.6 kcal/mol and 19.1 kcal/mol, respectively. The O1–H1 distances are 1.69 Å and 1.89 Å in the respective transition states (Fig. 5e). The enhanced protonation rates arise from the increased acidity of pTSA in the presence of three HFIP molecules, which form strong hydrogen bonds with the oxygens of pTSA. Subsequently, the proton at the C3 position of indole is abstracted by [pTSA][−], leading to aromatization of indole. The activation free energy of the aromatization step is 6.6 and −3.8 kcal/mol via **TS(B-P)_{pTSA}** and **TS(B-P)_{pTSA-3HFIP}** in implicit and explicit solvent models, respectively (Fig. 5d). This data suggests that HFIP not only participates as a solvent but also directly plays an important role in lowering down the barrier of nucleophilic attack of indole on activated ABB, followed by aromatization of indole. We also explored alternative reaction pathways, including interaction of the carbonyl group of ABB with a fourth HFIP molecule via **TS(A-B)_{pTSA-4HFIP}**, as well as uncatalyzed and ionic mechanisms. However, all these pathways were found to be associated with prohibitively high energy barriers that are not accessible under room-temperature conditions (see Supplementary information, Section 20, page S213). We also checked the barrier of nucleophilic attack of indole via **TS(A-B)_{pTSA}** in DCM, isopropanol, and ethanol solvents; the activation free-energy barriers for nucleophilic attack in these solvents were found to be high, i.e., 26.1, 28.2, and 24.0 kcal/mol, respectively. (see Supplementary Information, Section 20 and Table S7, page S212).

Synthetic application

The 1,3,4,9-tetrahydropyrano[3,4-*b*]indole is a key scaffold present in numerous marketed drugs and bioactive molecules. Its importance can be understood by the successful development of the potent anti-inflammatory drug (S)-Etodolac⁵⁰ and the long-acting non-narcotic analgesic agent pemedolac⁵¹. Our target was to access azetidine

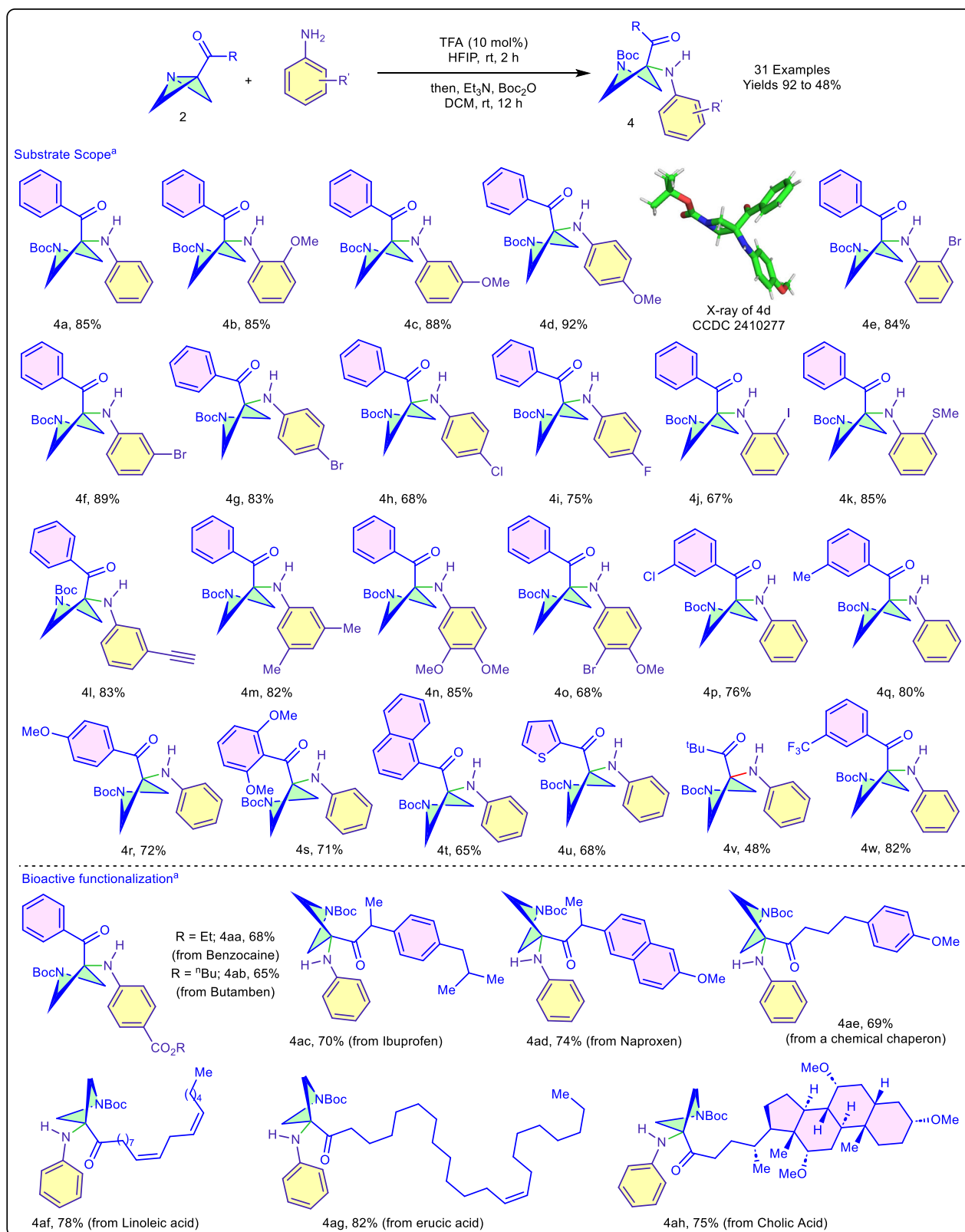


Fig. 4 | Substrate scope for nucleophilic ring opening of ABB using aniline as nucleophile; installation of aza-azetidine in marketed drugs, bioactive molecules, and fatty acids. [a] Reaction condition: 2 (0.2 mmol), aniline (0.4 mmol), TFA (10 mol%), HFIP (0.2 mL), after removal of HFIP add Et₃N (0.8 mmol), Boc₂O (0.4 mmol), DCM (5 mL).

tethered isochroman derivatives, which have not been explored previously. To achieve our goal, we have performed sodium borohydride-mediated reduction of the indole-azetidines to synthesize a series of azetidine-tethered secondary tryptophol (5). Acid-catalyzed oxa-

Pictet-Spengler reaction of these tryptophol derivatives with acetal gives us access to these azetidine-tethered indole-based isochroman derivatives 6 (Fig. 6a). We have explored the scope of this reaction; different tryptophols react with the acetal of benzaldehyde or *p*-

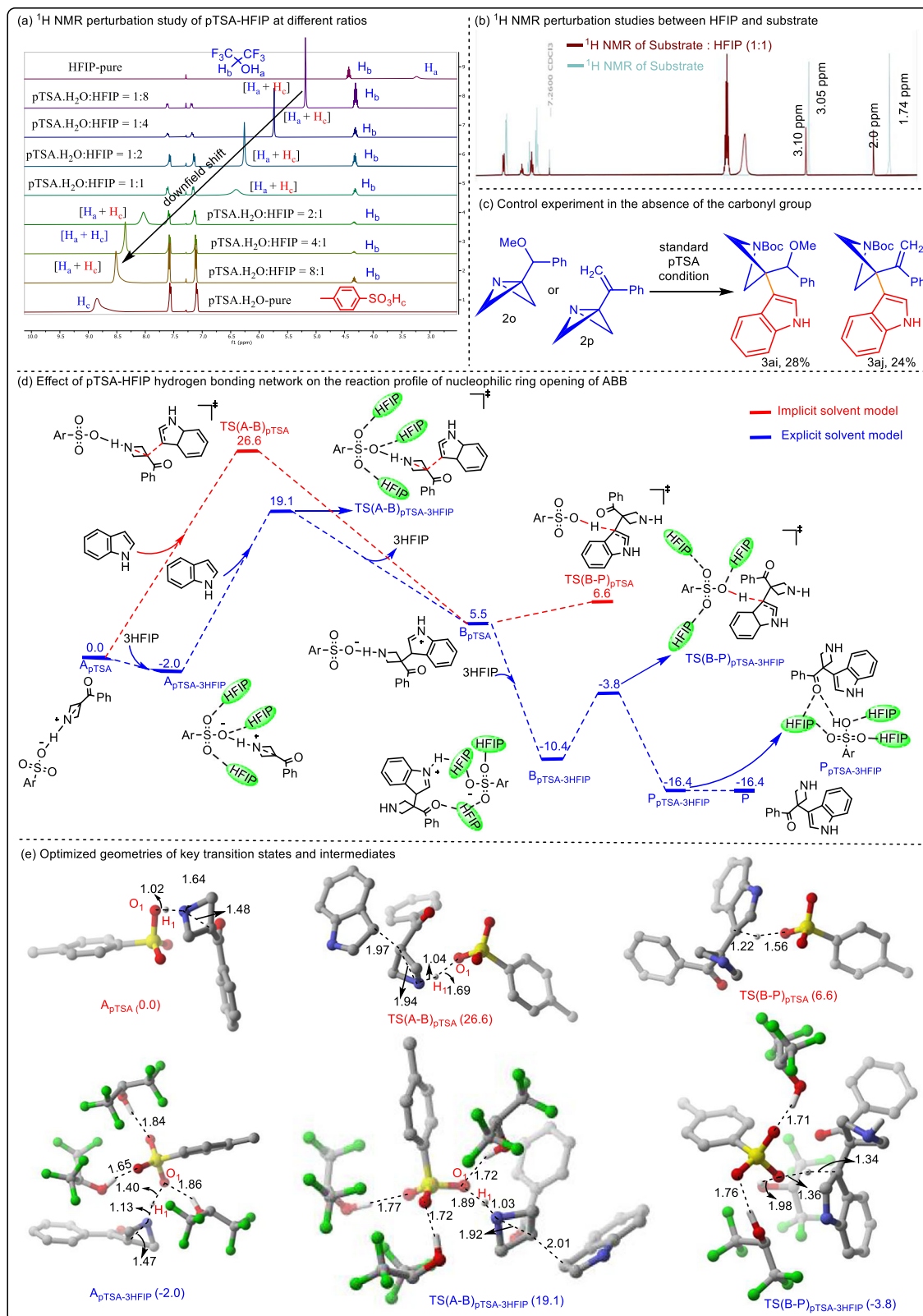


Fig. 5 | Mechanistic study. **a** ^1H NMR perturbation study of pTSA-HFIP at different ratios. **b** ^1H NMR perturbation studies between HFIP and substrate. **c** Control experiment in the absence of the carbonyl group. **d** Effect of pTSA-HFIP hydrogen

bonding network on the reaction profile of nucleophilic ring opening of ABB. **e** Optimized geometries of key transition states and intermediates.

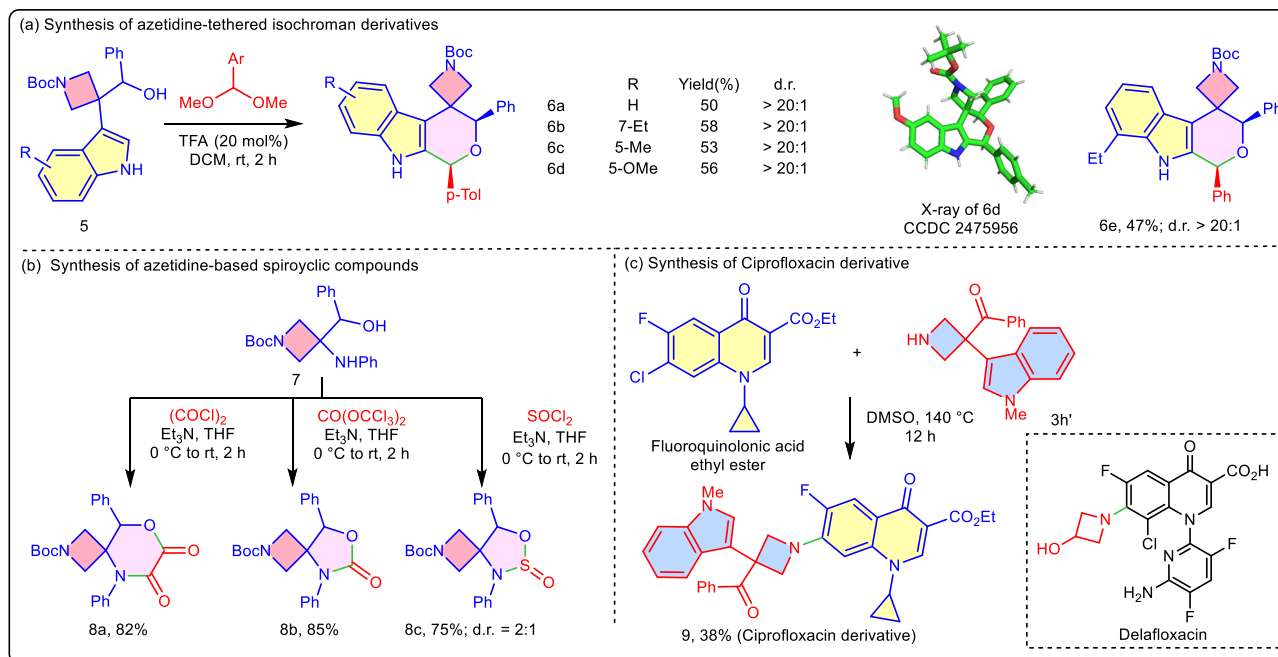


Fig. 6 | Synthetic application. **a** Synthesis of azetidine-tethered isochroman derivatives. **b** Synthesis of azetidine-based spirocyclic compounds. **c** Synthesis of ciprofloxacin derivative.

tolualdehyde to give the corresponding isochroman derivatives with moderate yield and excellent diastereoselectivity (*d.r.* > 20:1). The geometry of the major diastereomer was determined by X-ray crystallography of compound **6d**. Similarly, we have performed the reduction of the aniline-based aza-azetidines to access the corresponding amino alcohol (**7**). The amino alcohol reacts with oxalyl chloride, triphosgene, and thionyl chloride in the presence of triethylamine to give access to different spirocyclic compounds with very good isolated yield (Fig. 6b).

Ciprofloxacin is a common fluoroquinolone antibiotic used to treat several bacterial infections. One of the key synthetic approaches to synthesize ciprofloxacin involves nucleophilic *ipso*-substitution of the chlorine atom of fluoroquinolonic acid using piperazine as a nucleophile. Azetidine-based Ciprofloxacin analog delafloxacin has been approved as an antibiotic on the market. Researchers are mimicking this approach for the synthesis of ciprofloxacin derivatives by using suitable amines. We have also applied a similar concept, by heating fluoroquinolonic acid ethyl ester and indole-azetidine (**3h'**) in DMSO at 140 °C for 12 h, the ciprofloxacin derivative (**9**) was isolated in 38% yield (Fig. 6c). This result indicates the possibility of making a library of compounds for future antibacterial studies.

Gram-scale synthesis and recyclability of HFIP

The high cost of HFIP is a significant challenge for the large-scale synthesis of the developed protocol. To resolve this issue, we have checked the reuse and recyclability of HFIP solvent (see Supplementary Information, Section 7). We have performed the gram-scale synthesis of both *N*-Boc indole-azetidine (**3a**) and aniline-based *N*-Boc aza-azetidine (**4a**) by using 1.6 g (10 mmol) of benzoylated ABB and 10 mL of HFIP in each case (see Supplementary Information, Section 7). In the case of indole-azetidine, 2.94 g (78% yield) of the desired product was obtained, and 7 mL HFIP was recovered, whereas in the other case, 2.82 g (80% yield) of the desired aza-azetidine was obtained, and 7.5 mL HFIP was recovered. In both cases, recovered HFIP was used for two more cycles for the respective reactions, and this has a minimal effect on the yield (for indole-azetidine **3a**: 75% and 70%; for aza-azetidine **4a**: 76% and 72%) of the developed protocol (see Supplementary Information, Section 7).

Antibacterial sensitivity

The compounds containing the azetidine ring are reported to possess antibacterial activity against several strains of both gram-positive and gram-negative bacteria⁵². This fact led us to speculate on the possible antibacterial activity of the above-mentioned compounds containing the azetidine moiety. For a preliminary study, we picked a few aza-azetidine and indole-azetidine compounds. Soon, we realized that the indole-azetidine (**3a'**) showed excellent antibacterial properties (Fig. 7). We performed a broth microdilution assay three times to check the sensitivity of those compounds against DH5-Alpha *Escherichia coli* and *S. aureus* MTCC 1430, representatives of gram-negative and gram-positive bacteria, respectively. The bacteria were incubated in the absence or presence of these three compounds at a final concentration of 50 µg/mL for 18 hours at 36.5 °C. Our compounds were found completely ineffective against DH5-Alpha *E. coli* (Fig. 7C). However, in the case of *S. aureus* MTCC 1430, no growth was observed in the presence of **3a'** (Fig. 7B). Other indole-azetidine compounds included in this study are found to be ineffective. This result indicates that **3a'** may possess the potential to be an antibacterial agent against gram-positive bacteria, e.g., *S. aureus* MTCC 1430.

Determination of MIC

To further validate our observation and to assess the antibacterial property quantitatively, the minimum inhibitory concentration (MIC) assay against *S. aureus* MTCC 1430 was performed (Fig. 7A). To gain more insight into the structure-activity relationship, several analogs of **3a'** were also tested, which included *N*-Boc-protected indole-azetidine (**3a**) or *N*-Me indole-based indole-azetidine (**3h** and **3h'**) and the 5-methoxy indole analogue (**3c'**). Chloramphenicol, the well-known marketed antibiotic against *S. aureus*, was used as a positive control to compare the effectiveness with these test compounds. The experimental procedure is discussed in detail in the “Methods” section (see Supplementary Information, Section 14). In the MIC assay, it was observed that **3h**, **3h'**, and **3c'** were found ineffective against *S. aureus* MTCC 1430 (Fig. 7A), whereas **3a** was found to be mildly effective. Surprisingly, **3a'** exhibited higher antibacterial activity compared to that of Chloramphenicol. The MIC value of **3a'** was 10 µg/mL, whereas

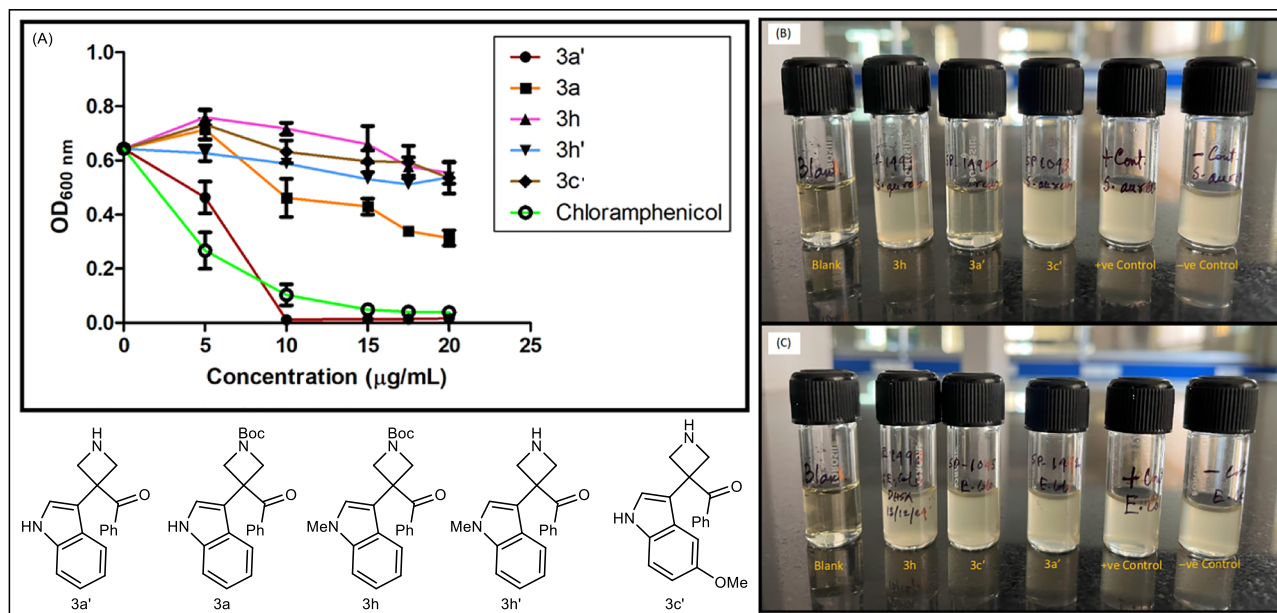


Fig. 7 | Antibacterial sensitivity study. **A** The minimum inhibitory concentration (MIC) against Gram-positive bacteria (*S. aureus* MTCC1430) was determined. Each set represents the MIC assay in the presence of five different novel test compounds and Chloramphenicol antibiotic (positive control). The bacterial growth data are presented as mean values \pm SEM of optical density at 600 nm. Error bars signify the standard error of the mean (SEM) for experiments performed in three biological replicates. Red graph with (●), orange graph with (■), pink graph with (▲), blue graph with (▼), brown graph with (◆) and green graph with (○) represent assay in varying concentration of 3a', 3a, 3h, 3h', 3c' (structures are exhibited in lower panel) and Chloramphenicol, respectively. It was observed that 3h, 3h', and 3c' were found ineffective against *S. aureus*. Whereas 3a showed mild bacterial growth inhibition compared to 3a', which showed the highest growth inhibition, even better than that of Chloramphenicol—the well-known marketed antibiotic. The determined MIC

value of Chloramphenicol was 19.17 ± 1.4 μ g/mL, whereas the determined MIC of 3a' compound was 10 μ g/mL. **B** Antibacterial sensitivity test of 3h, 3a', 3c' against gram-positive bacteria (*S. aureus* MTCC 1430). 'Blank' tube contained only Mueller Hinton broth (MHB), the other three experimental tubes marked as 3h, 3a' and 3c' contained 50 μ g/mL of test compounds, i.e., 3h, 3a' and 3c', respectively, in MHB and bacteria of 0.5 McFarland standard. None of the tested compounds was able to inhibit bacterial growth, except 3a'. +ve (positive) control tube contained bacteria in MHB. -ve (negative) control contained bacteria in 5% of DMSO and MHB. **C** Antibacterial sensitivity test of 3h, 3c', 3a' against gram-negative bacteria (*E. coli* DH5-Alpha). Blank, +ve control, -ve control, and the concentration of tested compounds were the same as in (B). None of these compounds exhibited bacterial growth inhibition in the case of gram-negative bacteria.

the MIC value of Chloramphenicol was 19.17 ± 1.4 μ g/mL. This result suggests that **3a'** can be used as a potential antibiotic candidate against *S. aureus* and other gram-positive bacteria in the future. From the structure-activity relationship study, we can say that the presence of an unsubstituted indole ring along with the unprotected azetidine group might play a determining role in the antibacterial property against Gram-positive bacteria.

To conclude, we have demonstrated a HFIP-assisted, Brønsted acid-catalyzed strain-release-driven ring-opening strategy to access aza-azetidines and indole-azetidines with a C3-quaternary center in excellent yield; a broad chemical space of significant medicinal relevance in terms of scaffold hopping via bioisosteric replacement. A broad range of indole, aniline, pyrrole, imidazole, triazole, and tetrazole have been shown to be compatible as nucleophiles. More than 60 examples of diversely substituted aza-azetidines and indole-azetidines have been synthesized to demonstrate their synthetic utility in a drug discovery context. Modular installation of aza-azetidine and indole-azetidine in bioactive molecules, marketed drugs, and natural products offers an alternative design strategy for medicinal chemists. The mechanistic pathway has been investigated with the help of DFT studies to establish the role of the hydrogen bonding network responsible for the reaction outcome. Preliminary bioactivity studies confirmed that indole-azetidine **3a'** has excellent antibacterial activity against the gram-positive bacteria *S. aureus*. The ADMET analysis confirmed the druggability of compound **3a'** (Supplementary Information, Table S3). Further antibacterial activity studies are ongoing to find a lead candidate against various other gram-positive and gram-negative bacteria. Considering aza-azetidine and indole-azetidine as bioisosteres of

piperazine and tryptamine, respectively, a scaffold-hopping strategy in those life-saving drugs will open a broad scope in medicinal chemistry, finding better drugs for tomorrow.

Methods

In an oven-dried reaction vial, benzoylated ABB (0.2 mmol, 1 eq.), indole or other *N*-heterocycle (0.4 mmol, 2 eq.), pTSA.H₂O (10 mol %), and hexafluoroisopropanol (0.2 mL) were taken and stirred for 24 h at room temperature. After full consumption of the benzoylated ABB, hexafluoroisopropanol was removed under reduced pressure. Then dry DCM (5 mL), Et₃N (0.8 mmol, 4 eq.), and di-*tert*-butyl dicarbonate (0.4 mmol, 2 eq.) were added sequentially and stirred overnight at room temperature. Then the solvent was removed under reduced pressure and purified by silica gel column chromatography.

In an oven-dried reaction vial, benzoylated ABB (0.2 mmol, 1 eq.), aniline (0.4 mmol, 2 eq.), TFA (10 mol%), and hexafluoroisopropanol (0.2 mL) were taken and stirred for 2 h at room temperature. After full consumption of the benzoylated ABB, hexafluoroisopropanol was removed under reduced pressure. Then dry DCM (5 mL), Et₃N (0.8 mmol, 4 eq.), and di-*tert*-butyl dicarbonate (0.4 mmol, 2 eq.) were added sequentially and stirred overnight at room temperature. Then the solvent was removed under reduced pressure and purified by silica gel column chromatography.

Reporting summary

Further information on research design is available in the Nature Portfolio Reporting Summary linked to this article.

Data availability

The data supporting the results of this work are included in this paper or in the Supplementary Information and are also available upon request from the corresponding author. Crystallographic data for the structures reported in this Article have been deposited at the Cambridge Crystallographic Data Centre, under deposition numbers CCDC 2410551 (for 3a), 2410278 (for 3v), 2410277 (for 4d), and 2475956 (for 6d). Copies of the data can be obtained free of charge via <https://www.ccdc.cam.ac.uk/structures/>. The coordinates of the optimized structure have been provided in the Source Data. Source data are provided with this paper.

References

1. Sun, H., Tawa, G. & Wallqvist, A. Classification of scaffold-hopping approaches. *Drug Discov. Today* **17**, 310–324 (2012).
2. Grisoni, F. et al. Scaffold hopping from natural products to synthetic mimetics by holistic molecular similarity. *Commun. Chem.* **1**, 44–52 (2018).
3. Tanabe et al. A novel in silico scaffold-hopping method for drug repositioning in rare and intractable diseases. *Sci. Rep.* **13**, 19358–19372 (2023).
4. Maienfisch, P. & Lamberth, C. Introduction to bioisosteric replacement and scaffold hopping in crop protection research. *Agric. Food Chem.* **70**, 10941 (2022).
5. Hu, Y., Stumpfe, D. & Bajorath, J. Recent advances in scaffold hopping. *J. Med. Chem.* **60**, 1238–1246 (2017).
6. Klein, H. F., Hamilton, D. J., de Esch, I. J. P., Wijnmans, M. & O'Brien, P. Escape from planarity in fragment-based drug discovery: a synthetic strategy analysis of synthetic 3D fragment libraries. *Drug Discov. Today* **27**, 2484–2496 (2022).
7. Tsien, J., Hu, C., Merchant, R. R. & Qin, T. Three-dimensional saturated C(sp³)-rich bioisosteres for benzene. *Nat. Rev. Chem.* **8**, 605–627 (2024).
8. Parmar, D. R. et al. Azetidines of pharmacological interest. *Arch. Pharm.* **354**, e2100062 (2021).
9. Kirichok, A. A. et al. “Angular” spirocyclic azetidines: synthesis, characterization, and evaluation in drug discovery. *Angew. Chem. Int. Ed.* **64**, e202418850 (2024).
10. Johnson, G. & Nichols, D. E. Indoloazetidines and Their Use in Methods for Treating 5-HT2 Responsive Conditions. PCT/US2022/026484. <https://patents.google.com/patent/WO2022232233A1/fr> (2022).
11. Kumar, A. et al. Nitrogen containing heterocycles as anticancer agents: a medicinal chemistry perspective. *Pharmaceuticals* **16**, 299–366 (2023).
12. Venail, F. et al. Safety, tolerability, pharmacokinetics and pharmacokinetic-pharmacodynamic modelling of the novel H4 receptor inhibitor SENS-111 using a modified caloric test in healthy subjects. *Br. J. Clin. Pharmacol.* **84**, 2836–2848 (2018).
13. Meanwell, N. A. & Loiseleur, O. Applications of isosteres of piperazine in the design of biologically active compounds: part 2. *J. Agric. Food Chem.* **70**, 10972–11004 (2022).
14. Kuramoto, Y. et al. A novel antibacterial 8-chloroquinolone with a distorted orientation of the N1-(5-amino-2,4-difluorophenyl) group. *J. Med. Chem.* **46**, 1905–1917 (2003).
15. Romanelli, M. N. et al. Synthetic approaches to piperazine-containing drugs approved by FDA in the period of 2011–2023. *Molecules* **29**, 68–116 (2024).
16. Mowbray, C. E. et al. Challenges of drug discovery in novel target space. The discovery and evaluation of PF-3893787: a novel histamine H4 receptor antagonist. *Bioorg. Med. Chem. Lett.* **21**, 6596–6602 (2011).
17. Yang, L., Hou, A., Jiang, Q., Cheng, M. & Liu, Y. Methodological development and applications of tryptamine-ynamide cyclizations in synthesizing core skeletons of indole alkaloids. *J. Org. Chem.* **88**, 11377–11391 (2023).
18. Van der Kolk, M. R., Janssen, M. A. C. H., Rutjes, F. P. J. T. & Blanco-Ania, D. Cyclobutanes in small-molecule drug candidates. *Chem-MedChem* **17**, e202200020 (2022).
19. Bull, J. A., Croft, R. A., Davis, O. A., Doran, R. & Morgan, K. F. Oxetanes: recent advances in synthesis, reactivity, and medicinal chemistry. *Chem. Rev.* **116**, 12150–12233 (2016).
20. Rojas, J. J. et al. Amino-oxetanes as amide isosteres by an alternative defluorosulfonylative coupling of sulfonyl fluorides. *Nat. Chem.* **14**, 160–169 (2022).
21. Gregson, C. H. U., Noble, A. & Aggarwal, V. K. Divergent, strain-release reactions of azabicyclo[1.1.0]butyl carbinols: semipinacol or spiroepoxy azetidine formation. *Angew. Chem. Int. Ed.* **60**, 7360–7365 (2021).
22. Jaiswal, V., Mondal, S., Singh, B., Singh, V. P. & Saha, J. Cation-promoted strain-release-driven access to functionalized azetidines from azabicyclo[1.1.0]butanes. *Angew. Chem. Int. Ed.* **62**, e202304471 (2023).
23. Gianatassio, R. et al. Strain-release amination. *Science* **351**, 241–246 (2016).
24. Lopchuk, J. M. et al. Strain-release heteroatom functionalization: development, scope, and stereospecificity. *J. Am. Chem. Soc.* **139**, 3209–3226 (2017).
25. West, M. S., Gabbey, A. L., Huestis, M. P. & Rousseaux, S. A. L. Ni-catalyzed reductive cross-coupling of cyclopropylamines and other strained ring NHP esters with (hetero)aryl halides. *Org. Lett.* **24**, 8441–8446 (2022).
26. Kozikowski, A. P. & Fauq, A. H. Synthesis of novel four-membered ring amino acids as modulators of the N-methyl-D-aspartate (NMDA) receptor complex. *Synlett* **11**, 783–784 (1991).
27. Symes, O. L. et al. Harnessing oxetane and azetidine sulfonyl fluorides for opportunities in drug discovery. *J. Am. Chem. Soc.* **146**, 35377–35389 (2024).
28. Singh, B., Sasmal, P., Taites, A., Hazra, S. & Saha, J. Aza-ortho-quinone methide promoted strain-release-driven conversion of azabicyclo[1.1.0]butanes into functionalized azetidines. *Org. Lett.* **26**, 9558–9563 (2024).
29. Bartnik, R. & Marchand, A. P. Synthesis and chemistry of substituted 1-azabicyclo[1.1.0]butanes. *Synlett* **9**, 1029–1039 (1997).
30. Hortmann, A. G. & Robertson, D. A. 1-Azabicyclobutanes. Synthesis and reactions. *J. Am. Chem. Soc.* **94**, 2758–2765 (1972).
31. Andresini, M., Degennaro, L. & Luisi, R. The renaissance of strained 1-azabicyclo[1.1.0]butanes as useful reagents for the synthesis of functionalized azetidines. *Org. Biomol. Chem.* **18**, 5798–5810 (2020).
32. Funke, W. Synthesis and properties of 1-azabicyclo[1.1.0]butanes. *Angew. Chem. Int. Ed. Engl.* **8**, 70–71 (1969).
33. Hsu, C.-M. et al. Azetidines with all-carbon quaternary centers: merging relay catalysis with strain release functionalization. *J. Am. Chem. Soc.* **145**, 19049–19059 (2023).
34. Ji, Y., Wojtas, L. & Lopchuk, J. M. An improved, gram-scale synthesis of protected 3-haloazetidines: rapid diversified synthesis of azetidine-3-carboxylic acids. *Arkivoc* **iv**, 195–214 (2018).
35. Wearing, E. R. et al. Visible light-mediated aza Paternò-Büchi reaction of acyclic oximes and alkenes to azetidines. *Science* **384**, 1468–1476 (2024).
36. Trauner, F. et al. Strain-release arylations for the bis-functionalization of azetidines. *Chem. Commun.* **58**, 2564–2567 (2022).
37. Tyler, J. L. & Aggarwal, V. K. Synthesis and applications of bicyclo[1.1.0]butyl and azabicyclo[1.1.0]butyl organometallics. *Chem. Eur. J.* **29**, e202300008 (2023).
38. Tyler, J. L., Noble, A. & Aggarwal, V. K. Four-component strain-release-driven synthesis of functionalized azetidines. *Angew. Chem. Int. Ed.* **61**, e202214049 (2022).
39. Rodríguez, R. I. et al. Radical strain-release photocatalysis for the synthesis of azetidines. *Nat. Catal.* **7**, 1223–1231 (2024).

40. Mlostoni, G. & Celeda, M. Ring opening of 1-azabicyclo[1.1.0]butanes with hydrazoic acid a facile access to *N*-unsubstituted azetidin-3-amines. *HCA* **88**, 1658–1663 (2005).
41. Motiwala, H. F. et al. HFIP in organic synthesis. *Chem. Rev.* **122**, 12544–12747 (2022).
42. Grant, P. S., Vavrik, M., Porte, V., Meyrelles, R. & Maulide, N. Remote proton elimination: C–H activation enabled by distal acidification. *Science* **384**, 815–820 (2024).
43. To, T. A., Pei, C., Koenigs, R. M. & Nguyen, T. V. Hydrogen bonding networks enable Brønsted acid-catalyzed carbonyl-olefin metathesis. *Angew. Chem. Int. Ed.* **61**, e202117366 (2022).
44. To, T. A., Phan, N. T. A., Mai, B. K. & Nguyen, T. V. Controlling the regioselectivity of the bromolactonization reaction in HFIP. *Chem. Sci.* **15**, 7187–7197 (2024).
45. Thai, P., Patel, L., Manna, D. & Powers, D. C. Hydrogen-bond activation enables aziridination of unactivated olefins with simple iminodiodanes. *Beilstein J. Org. Chem.* **20**, 2305–2312 (2024).
46. Singh, S., Mondal, S., Vodnala, N. & Hazra, C. K. Hydrogen bonding network-enabled Brønsted acid-catalyzed Friedel–Crafts reactions: a green approach to access unsymmetrical diaryl- and triarylmethanes. *Green. Chem.* **25**, 1014–1022 (2023).
47. Khan, J., Tyagi, A., Samanta, R. & Hazra, C. K. Chemoselective deoxygenative α -arylation of carboxylic acids, amides, and esters: synthesis of anesthetic and anti-inflammatory compounds. *Chem. Commun.* **60**, 10688–10691 (2024).
48. Kumar, S. Ritika. A brief review of the biological potential of indole derivatives. *Futur. J. Pharm. Sci.* **6**, 121 (2020).
49. Vuković, V. D., Richmond, E., Wolf, E. & Moran, J. Catalytic friedel–crafts reactions of highly electronically deactivated benzylic alcohols. *Angew. Chem. Int. Ed.* **56**, 3085–3089 (2017).
50. Lee, D. K. H. Effect of etodolac on the prostaglandin concentrations in the kidney of the normal rat. *Drug Dev. Res.* **9**, 305–311 (1986).
51. Katz, A. H. et al. Synthesis and analgesic activity of pemedolac [cis-1-ethyl-1,3,4,9-tetrahydro-4-(phenylmethyl)pyrano[3,4-b]indole-1-acetic acid]. *J. Med. Chem.* **31**, 1244–1250 (1988).
52. Kumura, K. et al. Synthesis and antibacterial activity of novel lincomycin derivatives. I. Enhancement of antibacterial activities by introduction of substituted azetidines. *J. Antibiot.* **69**, 440–445 (2016).

Acknowledgements

This work was supported by CSIR (O2(O431)/21/EMR-II) research grants. S.H. wants to thank IIT Kharagpur for the fellowship. T.D. and B.B. are thankful to DST-SERB, GOI (file no. SRG/2022/001543) for their financial assistance. A.T. thanks IISc Bangalore for the fellowship.

Author contributions

The project was supervised by S.P., and all the synthesis work was done by S.H. A.T. conducted the theoretical study under the supervision of G.J. T.D. conducted the biological study under the supervision of B.B. R.S. solved the X-ray crystal structure. S.P. and S.H. wrote the manuscript.

Competing interests

The authors declare no competing interests.

Additional information

Supplementary information The online version contains supplementary material available at <https://doi.org/10.1038/s41467-025-63680-z>.

Correspondence and requests for materials should be addressed to Santanu Panda.

Peer review information *Nature Communications* thanks the anonymous reviewer(s) for their contribution to the peer review of this work. A peer review file is available.

Reprints and permissions information is available at <http://www.nature.com/reprints>

Publisher's note Springer Nature remains neutral with regard to jurisdictional claims in published maps and institutional affiliations.

Open Access This article is licensed under a Creative Commons Attribution-NonCommercial-NoDerivatives 4.0 International License, which permits any non-commercial use, sharing, distribution and reproduction in any medium or format, as long as you give appropriate credit to the original author(s) and the source, provide a link to the Creative Commons licence, and indicate if you modified the licensed material. You do not have permission under this licence to share adapted material derived from this article or parts of it. The images or other third party material in this article are included in the article's Creative Commons licence, unless indicated otherwise in a credit line to the material. If material is not included in the article's Creative Commons licence and your intended use is not permitted by statutory regulation or exceeds the permitted use, you will need to obtain permission directly from the copyright holder. To view a copy of this licence, visit <http://creativecommons.org/licenses/by-nc-nd/4.0/>.

© The Author(s) 2025